

LETTER • OPEN ACCESS

## Why Pacific quasi-decadal oscillation has emerged since the mid-20th century

To cite this article: Chunhan Jin *et al* 2022 *Environ. Res. Lett.* **17** 124039

View the [article online](#) for updates and enhancements.

You may also like

- [CsPbCl<sub>3</sub> perovskite quantum dots/TiO<sub>2</sub> inverse opal photonic crystals for efficient photoelectrochemical detection of alpha fetoprotein](#)  
Jiaqiong Qin, Shaobo Cui, Xingqiang Yang et al.
- [Highly efficient silica-coated Eu<sup>3+</sup> and Mn<sup>2+</sup> doped CsPbCl<sub>3</sub> perovskite quantum dots for application in light-emitting diodes](#)  
Yinhua Wang, Yongsheng Zhu, Gang Yang et al.
- [Toward efficient photocatalysts for light-driven CO<sub>2</sub> reduction: TiO<sub>2</sub> nanostructures decorated with perovskite quantum dots](#)  
Yunju Liu, Chen-Chin Lee, Mark W Horn et al.

ENVIRONMENTAL RESEARCH  
LETTERS

## LETTER

## OPEN ACCESS

## RECEIVED

16 October 2022

## REVISED

21 November 2022

## ACCEPTED FOR PUBLICATION

30 November 2022

## PUBLISHED

9 December 2022

Original content from  
this work may be used  
under the terms of the  
[Creative Commons  
Attribution 4.0 licence](#).

Any further distribution  
of this work must  
maintain attribution to  
the author(s) and the title  
of the work, journal  
citation and DOI.

Why Pacific quasi-decadal oscillation has emerged since the  
mid-20th centuryChunhan Jin<sup>1,2</sup> , Bin Wang<sup>3,4,\*</sup> and Jian Liu<sup>5,6,7</sup><sup>1</sup> College of Geography and Remote Sensing Science, Xinjiang University, Urumqi 830046, People's Republic of China<sup>2</sup> Xinjiang Key Laboratory of Oasis Ecology, Xinjiang University, Urumqi 830046, People's Republic of China<sup>3</sup> Department of Atmospheric Sciences and International Pacific Research Center, School of Ocean and Earth Science and Technology, University of Hawaii at Manoa, Honolulu, HI 96825, United States of America<sup>4</sup> Earth System Modeling Center, Nanjing University of Information Science and Technology, Nanjing 210044, People's Republic of China<sup>5</sup> Key Laboratory for Virtual Geographic Environment of Ministry of Education/State Key Laboratory of Geographical Evolution of Jiangsu Provincial Cultivation Base/Jiangsu Center for Collaborative Innovation in Geographical Information Resource Development and Application, School of Geography Science, Nanjing Normal University, Nanjing 210023, People's Republic of China<sup>6</sup> Open Studio for the Simulation of Ocean-Climate-Isotope, Pilot National Laboratory for Marine Science and Technology, Qingdao 266237, People's Republic of China<sup>7</sup> Jiangsu Provincial Key Laboratory for Numerical Simulation of Large Scale Complex System, School of Mathematical Science, Nanjing Normal University, Nanjing 210023, People's Republic of China

\* Author to whom any correspondence should be addressed.

E-mail: [wangbin@hawaii.edu](mailto:wangbin@hawaii.edu)**Keywords:** Pacific quasi-decadal oscillation, ENSO, tropical Pacific decadal variability, multi-year La Niña events, 11-year solar cycle, climate simulations, CESM-LMESupplementary material for this article is available [online](#)

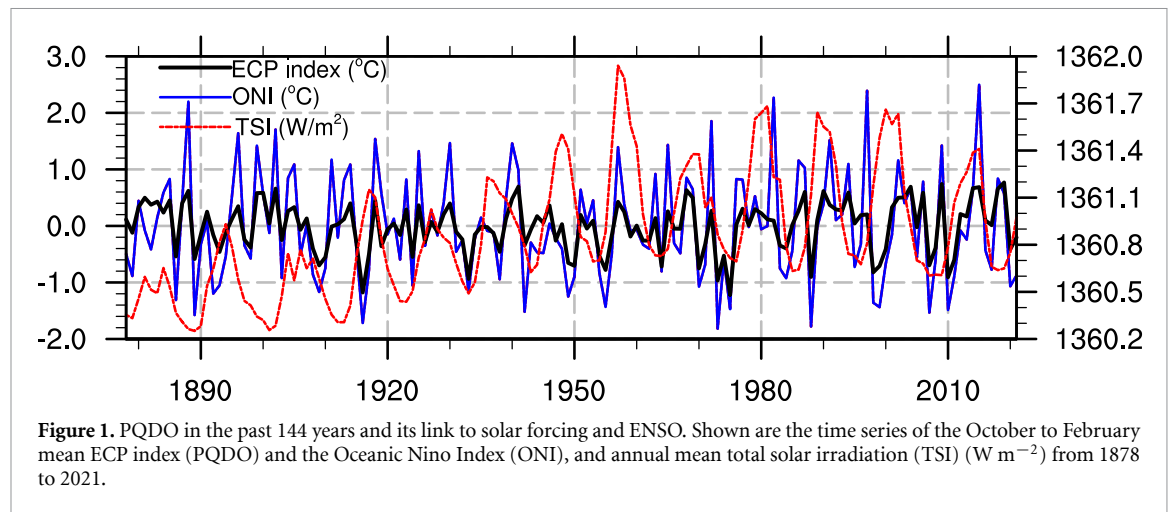
## Abstract

Pacific quasi-decadal oscillation (PQDO) is one component of the multi-time-scale tropical Pacific decadal variability, with a variability center in the equatorial central Pacific (ECP). PQDO has emerged since the 1950s and has a significant impact on decadal climate variability over Asia and North America and Pacific storms. However, why it has intensified since the 1950s remains unknown. Here we test two competing hypotheses, (1) 11-year solar cycle forcing and (2) internal variability arising from El Niño–Southern Oscillation (ENSO) asymmetry, by analyzing simulation results, including one fixed-forcing control (CTRL) experiment and four sensitive experiments with millennial spectral solar irradiance (SSI), obtained from the Community Earth System Model–Last Millennium Ensemble modeling project. The four-member ensemble-averaged SSI experiments suggest that 11-year solar irradiance forcing cannot excite PQDO without stratospheric amplification of solar forcing. By analyzing 144 years of observations and the CTRL experiment, we find that the PQDO is nonstationary, and consecutive La Niña-induced decadal variability can boost PQDO in the ECP. El Niño could induce decadal ENSO signals in the NINO3.4 region but not in PQDO regions. The negative phase of PQDO tends to follow the occurrence of multi-year La Niña. We suggest that the emergence of PQDO since the 1950s is mainly due to the increase in multi-year La Niña events.

## 1. Introduction

Tropical Pacific decadal variability (TPDV) has attracted a great deal of attention in the climate research community because of its profound impact on weather, agriculture, ecosystems and the economy (Power *et al* 2021). TPDV exhibits a variety of forms in terms of their temporal and spatial behaviors. Nevertheless, their complex causes remain uncertain. In

terms of time scales, three components have been identified. One is Pacific decadal oscillation, with two preferred periodicities (15–25 years and 50–70 years), most visible in the North Pacific (Mantua *et al* 1997). Another is Interdecadal Pacific Oscillation, covering the entire Pacific (Power *et al* 1999). The third is Pacific quasi-decadal oscillation (PQDO), which has a variability center over the equatorial central Pacific (ECP) with an 11-year periodicity; its



intensity is slightly weaker compared with the first two oscillations (Brassington 1997, Lyu *et al* 2017). PQDO has a significant impact on tropical cyclone activity, the Asian monsoon and North American continental climate anomalies (Wang *et al* 2014, Anderson *et al* 2016, Yue *et al* 2020).

PQDO is less studied than other components of TPDV. Knowledge about its characteristics and dynamics is still in the development stage. Jin *et al* (2021) documented the spatial–temporal characteristics of PQDO and found it to be an episodic-like quasi-decadal warm/cold event. It initially develops in a northeast–southwest tilted belt from the Californian coast to the ECP by off-equatorial atmosphere–ocean interaction, and it matures in the ECP. Thus, they represented PQDO by an ECP index defined by the sea surface temperature anomalies (SSTAs) averaged over  $10^{\circ}\text{S}$ – $10^{\circ}\text{N}$  and  $160^{\circ}\text{E}$ – $160^{\circ}\text{W}$ . They showed that ECP warming is amplified primarily due to equatorward heat advection and a deepening thermocline, while zonal advective feedback mainly controls its decay. This ECP development distinguishes it from El Niño–Southern Oscillation (ENSO) dynamics, in which thermocline–upwelling feedback dominates (Bjerkness 1969). However, the origin of PQDO remains controversial.

Some studies attribute PQDO to the response of Pacific sea surface temperature (SST) to the 11-year solar cycle (e.g. White and Liu 2008a, 2008b). To this end, three lines of thinking have been presented. The first postulates that a weak La Niña-like SSTa is generated during the solar peak year followed by an El Niño-like warming 1 to 2 years later (Van Loon *et al* 2007, Meehl and Arblaster 2009, Meehl *et al* 2009). The second proposes the opposite: a weak El Niño-like pattern occurs at the solar cycle maximum (Roy and Haigh 2010, Misios and Schmidt 2012, Misios *et al* 2019). The third suggests that a weak SST warming pattern in the ECP modulated by the solar cycle

leads to neither an La Niña-like nor an El Niño-like SST mode (Tung and Zhou 2010, Huo *et al* 2021). In addition, PQDO triggered by the solar cycle may depend on the magnitude and periodicity of the solar irradiance (White *et al* 1998, Drews *et al* 2021). How the equatorial Pacific SST responds to the 11-year solar cycle remains obscure.

PQDO could also occur as internal variability. Like other components of TPDV, PQDO shows a spatial structure similar to ENSO (Allan 2000, Tourre *et al* 2001, Allan *et al* 2003). Thus, TPDV, including PQDO, was linked to ENSO-like decadal variability generated by the mechanisms that operate through the interannual ENSO cycle (White *et al* 2003, Vimont 2005) or considered as a residual of ENSO events (Kim and Kug 2020, Power *et al* 2021). Recent studies have also focused on the interaction between ENSO and interdecadal Pacific variability (e.g. Kim and Kug 2020, Sun and Okumura 2020, Zhao and Di Lorenzo 2020). However, the relationship between ENSO and PQDO has not been fully understood.

Jin *et al* (2021) found PQDO to be a nonstationary phenomenon: it has emerged since 1950 but was absent between 1878 and 1950. As shown in figure 1, the 11-year solar cycle was also amplified after the 1950s, and PQDO tends to follow it with a 1–2-year phase delay, suggesting that solar forcing might affect PQDO. On the other hand, the properties of ENSO also experienced significant changes (Wang *et al* 2019). However, the origins of PQDO and why it has intensified since 1950 still need to be addressed.

This study explores the origin of PQDO by testing two competing hypotheses, whether PQDO is a forced response to total solar irradiance (TSI) or a manifestation of internal variability, especially the low-frequency variability associated with ENSO asymmetry. We also explore why PQDO became

strong in the most recent seven decades but not before (1878–1950).

## 2. Data and method

### 2.1. Observational data and definition of the indices

The observed monthly mean SST from 1878 to 2021 is merged from two SST datasets, including the Hadley Centre Sea Ice and Sea Surface Temperature (HadISST) (Rayner *et al* 2003) and the National Oceanic and Atmospheric Administration Extended Reconstructed SST (ERSST) version 5 (Huang *et al* 2017), by simply taking their arithmetic means.

PQDO is represented by the ECP index defined by the SSTAs averaged over a large area in the ECP ( $10^{\circ}$  S– $10^{\circ}$  N,  $165^{\circ}$  E– $165^{\circ}$  W) (Jin *et al* 2021). ENSO variability is measured by the Oceanic Niño index (ONI); namely, the SSTA averaged over the NINO3.4 region ( $5^{\circ}$  S– $5^{\circ}$  N,  $170^{\circ}$  W– $120^{\circ}$  W). A La Niña year is defined by ONDJF (October–November–December–January–February) with averaged ONI equal to or below  $-0.5^{\circ}$  C and an El Niño year is defined by ONDJF ONI equal to or above  $0.5^{\circ}$  C. Given the increasing trend in the present warming period, all the indices built from the observational data are detrended.

### 2.2. Validation of the Community Earth System Model's ENSO

Considering the difficulty in detecting forced signals from limited observations, we analyzed long-term numerical simulation data obtained from the Community Earth System Model–Last Millennium Ensemble (CESM-LME) modeling project (Otto-Bliesner *et al* 2016), including one fixed-forcing control (CTRL) experiment and four sensitivity experiments with spectral solar irradiance (SSI) for the period AD 850–2005.

To ensure that the model can reproduce reasonably realistic ENSO variability, we examined some aspects of the model performance, including ENSO phase locking to the annual cycle and El Niño–La Niña asymmetry. The asymmetry here means that El Niño has a larger amplitude than La Niña, but La Niña lasts longer than El Niño (An and Jin 2004, Okumura and Deser 2010).

The observed maximum standard deviation (SD) of the ONI occurs in December (figure S1), confirming ENSO mature phase locking to the end of the calendar year (Rasmusson and Carpenter 1982). Variability of the ONI reaches a minimum from May to June. The CESM-LME CTRL experiment generally captures the observed phase-locking of ENSO, although the simulation slightly overestimates the variance (figure S1, dotted line). CESM can reasonably reproduce the asymmetry in the

amplitudes of El Niño and La Niña. The simulated maximum magnitudes for El Niño and La Niña events are  $1.81^{\circ}$  C and  $-1.25^{\circ}$  C, which qualitatively match the observed  $1.30^{\circ}$  C and  $-1.14^{\circ}$  C, respectively.

It has been demonstrated that the first and second empirical orthogonal function (EOF) patterns of ENSO resemble the linear signal (SD) and nonlinear signal (skewness), respectively (Monahan and Dai 2004). The observed EOF1 features a typical mature ENSO-like pattern with the center located over the eastern-central Pacific and explains 70% of the total variance; EOF2 displays an east–west dipole pattern that characterizes the asymmetric aspect of ENSO variability (figure S2). The spatial patterns of EOF1 and EOF2 in the CTRL run are generally consistent with the observed patterns, although the eastern-central Pacific SSTAs in EOF1 extend westward by  $20^{\circ}$ – $30^{\circ}$  of longitude, which results from the cold tongue bias commonly seen in many models (Li *et al* 2016, Ying *et al* 2019). Despite the discrepancies, the model generally captures the observed ENSO asymmetry.

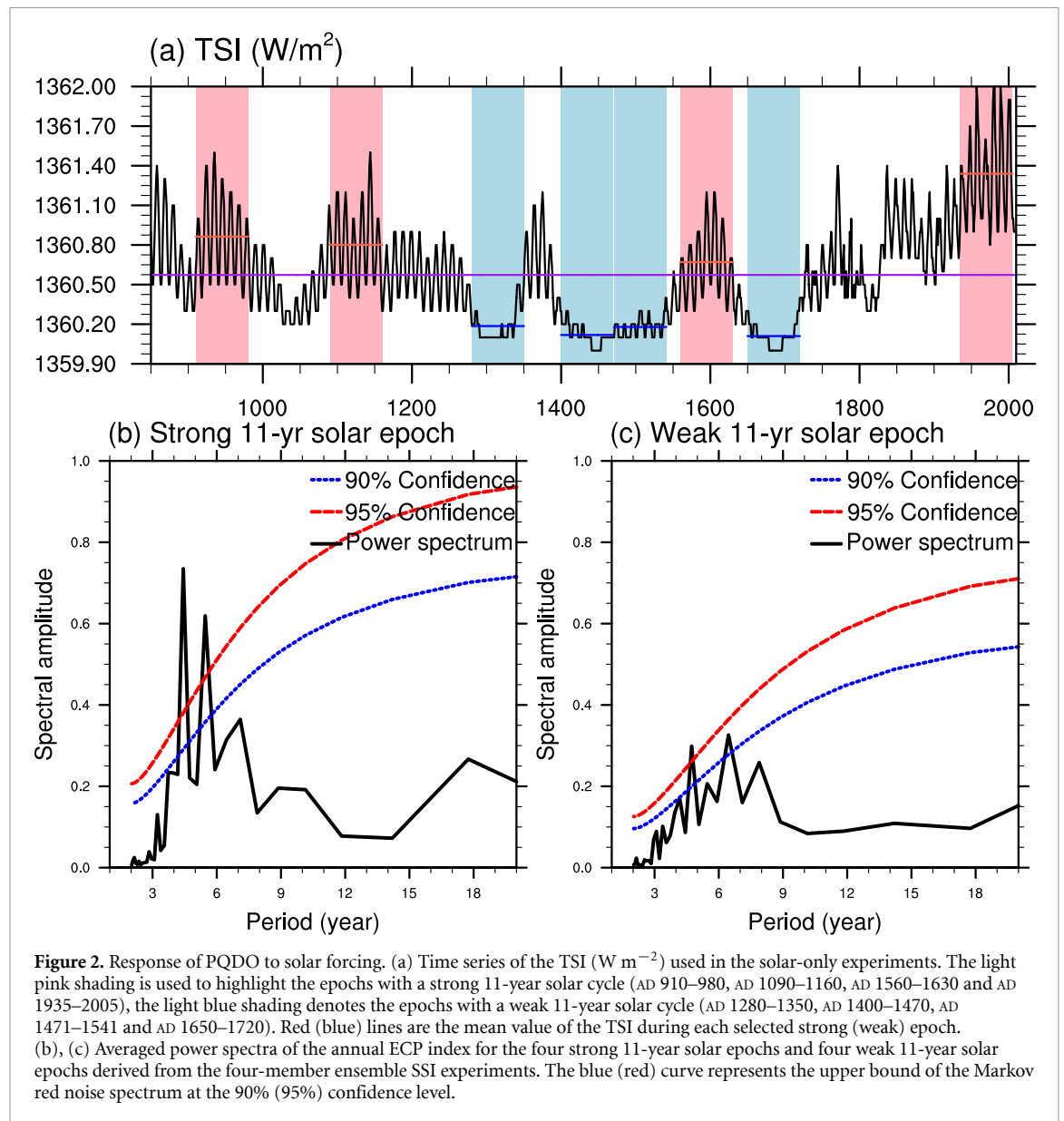
## 3. Results

### 3.1. PQDO response to 11-year solar irradiance forcing

There are four solar-forcing (SSI) experiments in which the model was driven by only time-varying solar irradiance forcing with an 11-year solar cycle (Vieira *et al* 2011), with all other external forcings being fixed at the AD 850 conditions. The TSI used in the SSI experiment is reconstructed by direct sunspot counts back to 1610 and an indirect record of solar activity from ice cores and tree rings for the longer TSI. Four SSI experiments allow for an ensemble mean that better represents a forced response by substantially reducing the internal variability. We examined the ensemble mean of four SSI experiments to investigate the responses of Pacific SST to different intensities (mean value) and variabilities (SD) of TSI forcing.

Based on the wavelet analysis of the TSI used in the SSI experiments (figure S3), we selected four equal-length (70 year) epochs with the strong 11-year solar cycle and four epochs with weak 11-year solar cycles, respectively (figure 2(a)). The averaged mean value and SD of the TSI during the four strong 11-year epochs are  $1360.92 \text{ W m}^{-2}$  and  $0.29 \text{ W m}^{-2}$ , respectively. These are larger than their counterparts during the four weak 11-year solar cycle epochs with a mean (SD) value of  $1360.15 (0.09) \text{ W m}^{-2}$ .

The power spectra of the annual ECP index measure the significance and intensity of PQDO. We analyzed the averaged spectra of the four strong (weak) 70-year epochs to detect the forced response to a strong (weak) 11-year solar cycle. The averaged power



spectra show similar spectral peaks for the strong and weak 11-year solar cycle epochs (figures 2(b) and (c)); both have significant peaks on a 4–7-year time scale. Notably, no significant forced decadal signals exist, suggesting that 11-year solar irradiance cycles could not excite PQDO in the model. The 4–7-year peak manifests residual ENSO variability in the central Pacific because the four-member ensemble mean could not completely remove ENSO signals. But the average substantially reduced the internally generated interannual variance by one order of magnitude compared with the peaks in the control run (figure 4(b)). The power spectra of the ONDJF ECP index derived from the SSI experiment present similar results. Results here provide evidence that the 11-year solar irradiance forcing cannot directly excite the ECP quasi-decadal oscillation, regardless of the strong 11-year solar cycle or the strong solar intensity and variability.

A cautious note is that this conclusion is derived from a single model, namely CESM. Previous

studies have speculated on the role of the top-down stratospheric amplification of the solar forcing in impacting Pacific SST variation acting together with a bottom-up coupled ocean–atmosphere response (Meehl *et al* 2009). However, the model used in the CESM-LME simulation does not have sufficient vertical resolution to resolve the stratospheric processes. Therefore, further studies with more sophisticated models are deemed necessary to assess the potential impacts of 11-year solar forcing on PQDO.

### 3.2. The links between PQDO and ENSO

#### 3.2.1. Temporal structures of PQDO and ENSO low-frequency variation

We start to explore the observed linkage between PQDO and ENSO by focusing on boreal winter (ONDJF), because both ENSO and PQDO mature during ONDJF. Given the ENSO phase asymmetry, our power spectra analysis of ONI is applied to La Niña-only (or El Niño-only) years. Therefore, we

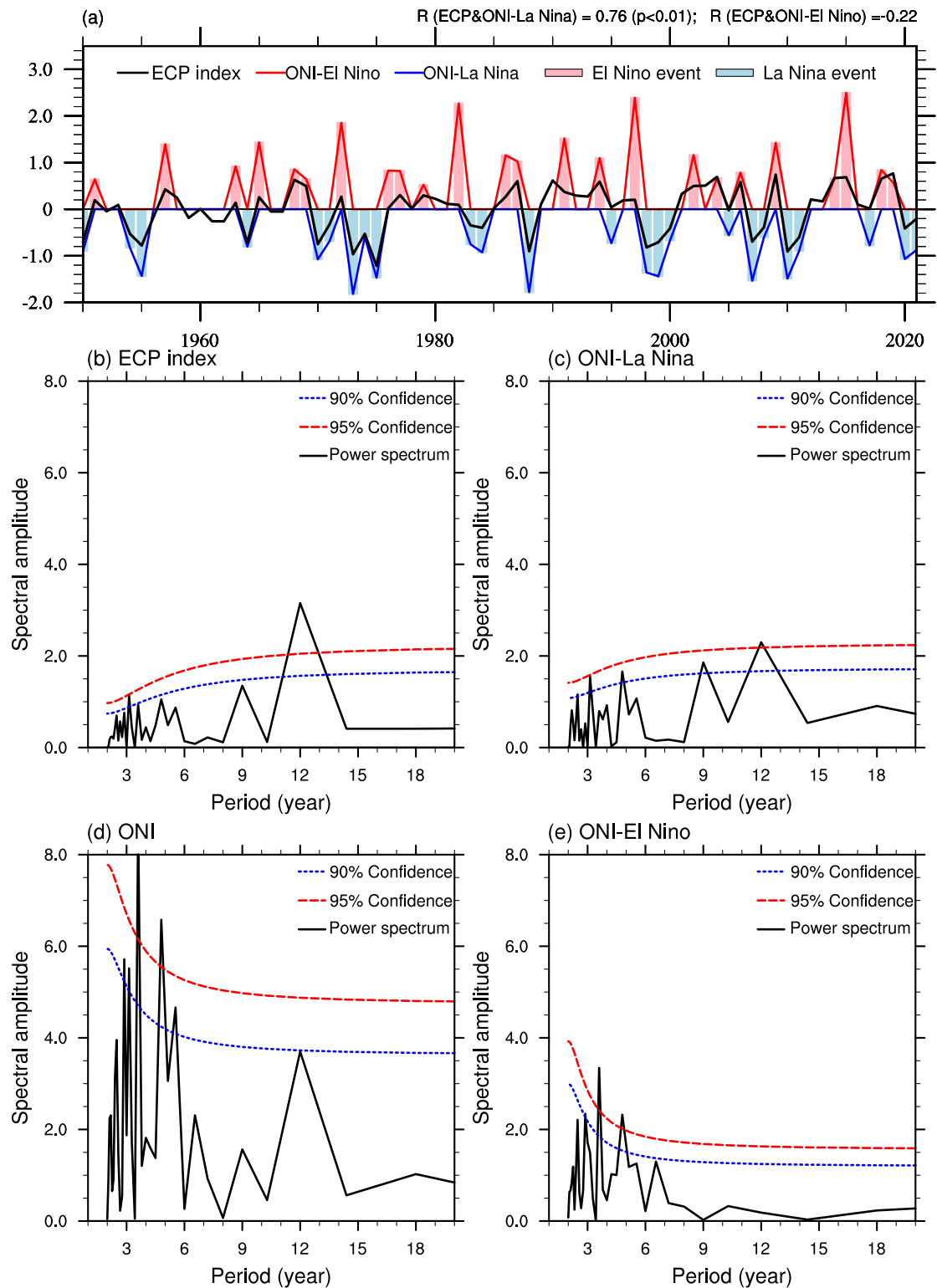


**Figure 3.** Observed contribution of El Niño and La Niña to PQDO. (a) Time series of the ECP index (black line), ONI-La Niña (blue line) and ONI-El Niño (red line) from 1950 to 2021. Light blue (light pink) histograms show La Niña (El Niño) events. The blue (red) curve denotes the ONI-El Niño (ONI-La Niña) index. The correlation coefficients between the ECP index with ONI-La Niña and ONI-El Niño are shown at the top-right corners. The power spectrum of (b) the ECP index, (c) ONI-La Niña, (d) ONI and (e) ONI-El Niño from 1950 to 2021. All indices are the ONDJF mean.

define two new indices (figure 3(a)). One is the ONI-El Niño, in which the ONI time series includes only El Niño years, and the neutral and La Niña years are replaced by zero. Another is ONI-La Niña, a time series that sets neutral and El Niño years to zero.

Figure 3(a) shows the time series of ONI-El Niño and ONI-La Niña. The motivation was to identify the contributions of El Niño and La Niña to PQDO. Note that if we set all negative (positive) values of the ONI as ONI-La Niña (ONI-El Niño), the obtained



power spectra are highly similar (figure not shown for brevity).

Let us examine what happened between 1950 and 2021 first. Interestingly, the ECP index and ONI-La Niña have nearly the same spectral peaks (figures 3(b) and (c)), and both have a significant 12-year peak ( $p < 0.05$ ). These results suggest that La Niña events have a prominent decadal signal beyond the interannual time scale that could contribute to PQDO. Additionally, the time series of ONI-La Niña is highly positively correlated with the ECP index with a correlation coefficient  $r = 0.76$ , an effective degree of freedom (EDF) of 23 and  $p < 0.01$ . In contrast, ONI-El Niño is insignificantly correlated with the ECP index with  $r = -0.22$  (EDF = 18), suggesting that La Niña makes a critical contribution to PQDO but El Niño does not. In calculating the correlation coefficient, we did not account for the neutral years, and the significance test used the EDF following Bretherton *et al* (1999).

The intimate linkage between PQDO and ONI-La Niña arises because La Niña's minimum SSTA is nearly collocated with PQDO in the ECP. Conversely, the El Niño events have maximum SSTA in the NINO3.4 region, coinciding with the maximum ONI. Thus, one might expect ONI to be linked to ONI-El Niño. It turns out that ONI and ONI-El Niño have almost the same spectral peaks on an interannual time scale but not on a decadal time scale (figures 3(d) and (e)). The quasi-12-year peak in the ONI is marginally significant ( $p = 0.1$ ), while the decadal signal is absent in ONI-El Niño. Hence, the ONI decadal peak is also related to a La Niña-generated decadal component.

How about the power spectra in observations before 1950? As shown in figure S4, the power spectra of the ECP index, ONI-La Niña, ONI and ONI-El Niño differ considerably from the results shown for 1950–2021. Between 1878 and 1949, the ECP index and ONI-La Niña have similar spectral peaks, except that ONI-La Niña has a significant 8-year peak, and ONI-El Niño shows a sharp 4-year peak that dominates the interannual variability of the ONI.

To test the findings obtained from observations, we analyze the CTRL experiment. In the CTRL experiment, the external forcing is fixed at AD 850 so that the climate variations of the models are produced by internal feedback processes within the coupled climate system. We selected a continuous 500-year sample from the CTRL experiment to study the temporal behaviors of ENSO and PQDO using the ONI and ECP indices. A wavelet analysis of the ECP index confirms that the model-simulated PQDO is non-stationary: it tends to be stronger in the first 250 years and weaker in the last 250 years. The ECP index and ONI share a similar power distribution on the interannual (2–7-year) time scale. However, the ECP

index has significant interdecadal (>16 years) variability which is absent in the ONI. The two equal-length (250 years) epochs provide a testbed for investigating the relationship between PQDO and ENSO.

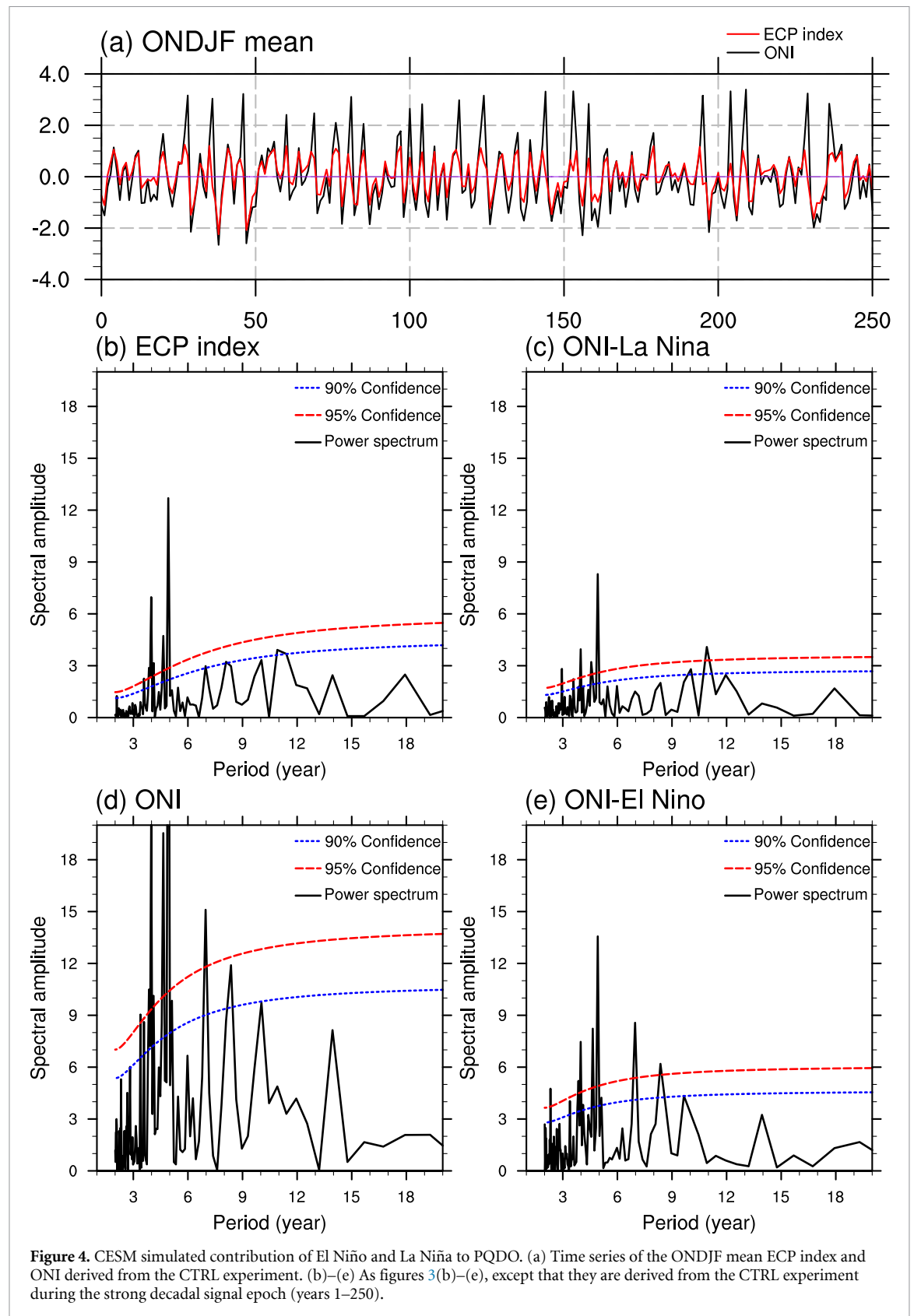
During the first 250 years, the magnitude of the positive ONI is much stronger than the negative ONI, reflecting the skewness of the ENSO cycle or ENSO phase asymmetry (figure 4(a)). Conversely, the ECP index is primarily symmetric between the magnitudes of the positive and negative anomalies. Thus, the negative ECP index generally coincides with negative ONI, but the positive ECP values are usually much lower than the positive ONI values. This feature corroborates the observed features, especially for 1950–2021 (figure 1). The power spectra of the ECP index, ONI-La Niña, ONI and ONI-El Niño derived from CTRL experiment during the first 250 years are generally consistent with the results shown for the strong PQDO epoch (1950–2021). The simulated ECP spectrum coincides with ONI-La Niña on the interannual and decadal time scales, with a significant 11-year periodicity. The ONI spectrum resembles ONI-El Niño, although the spectral amplitude of the ONI is much stronger than that for ONI-El Niño. Besides, the time series of ONI-La Niña is well positively correlated with that of the ECP ( $r = 0.86$ , EDF = 69,  $p < 0.01$ ). In contrast, the ONI-El Niño time series is negatively related to the ECP index with  $r = -0.41$  (EDF = 61).

An important point we want to make is that the low-frequency (decadal) ENSO produced by irregular occurrence of El Niño and La Niña is highly nonstationary in both periodicity and amplitude (Wittenberg 2009). This assertion is exemplified by what happened in the weak PQDO epoch (years 251–500) (figure S6). During that epoch, the ECP index and ONI-La Niña had very similar spectral peaks, but the decadal signal was absent, suggesting that the absence of the La Niña decadal signal leads to an inactive PQDO. On the other hand, ONI-El Niño shows a sharp 11-year peak that dominates the decadal variability of the ONI.

In sum, both La Niña and El Niño could produce a significant decadal component beyond the interannual. However, the two phases of ENSO, i.e. El Niño and La Niña, have different SST variability centers. Therefore, El Niño's decadal component can affect low-frequency ONI but not PQDO. In contrast, La Niña's decadal component mainly affects PQDO. ENSO phase asymmetry in SST variability centers plays a critical role in generating PQDO.

### 3.2.2. Evolution of the spatial structures of PQDO and ENSO low-frequency variation

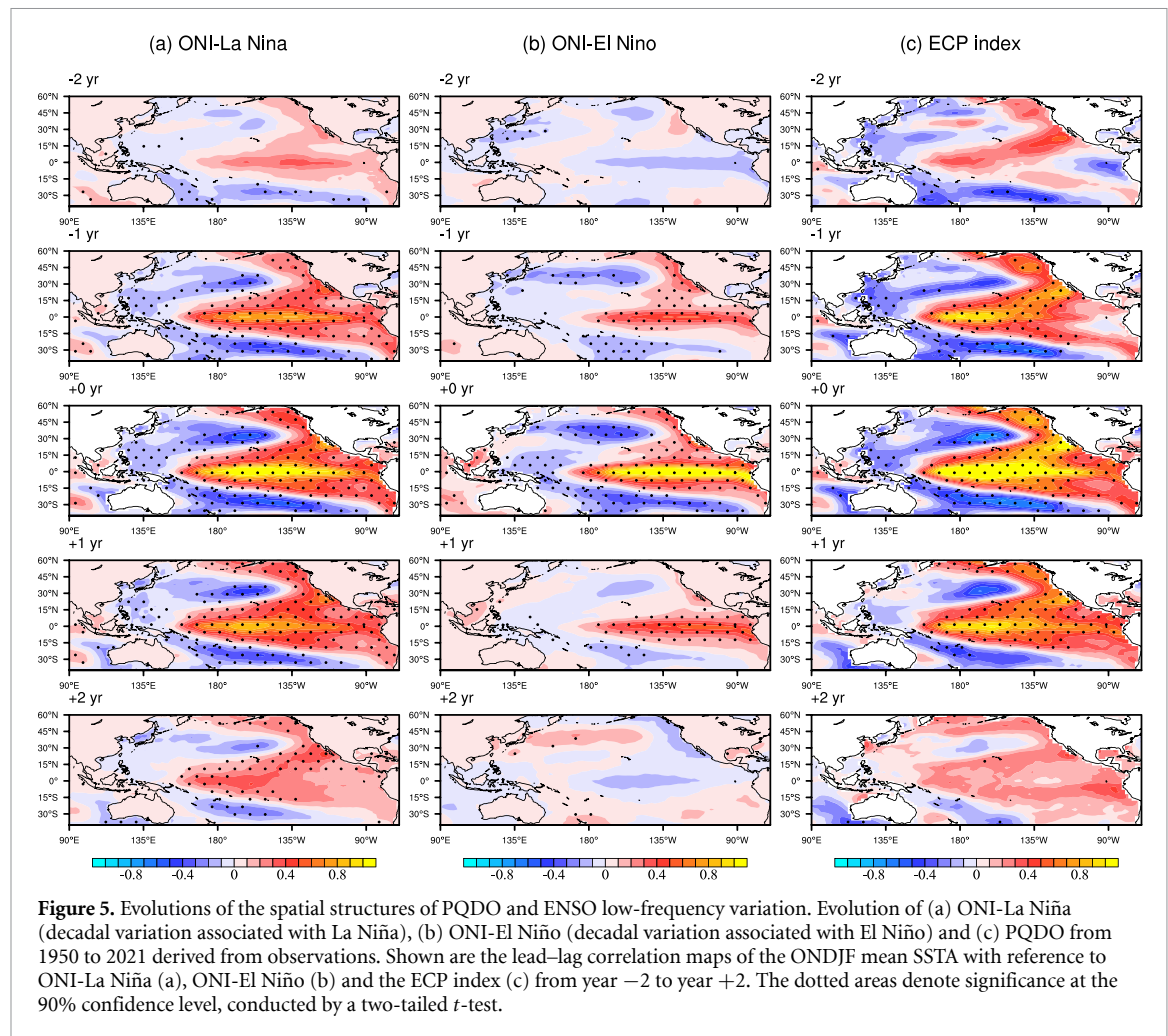
To investigate evolution of the spatial structures of the SSTAs associated with PQDO and the low-frequency ENSO, we used 3-year running ONDJF



SSTA to construct the lead-lag correlation maps with reference to the ECP index, ONI-La Niña and ONI-El Niño decadal variability from year  $-2$  to year  $+2$  derived from observation and the model's CTRL experiment (figures 5 and S7, S8). From 1951–2021 when PQDO was significant, ONI-La Niña

SST evolution differs significantly from El Niño-only evolution (figures 5(a) and (b)). ONI-La Niña has a longer life cycle, whereas ONI-El Niño is more like a short and smooth single event. The evolution of ONI-La Niña shows an expanded PDO-like pattern, while ONI-El Niño features a more equatorially





trapped pattern. The action center induced by La Niña's decadal variability is closer to the dateline than that caused by El Niño at year 0. Figure 5(c) shows PQDO evolution depicted by the SSTA evolution associated with the ECP index. The evolution of ONI-La Niña SST resembles PQDO evolution considerably better than ONI-El Niño, especially at year  $-2$  and year  $+2$ . ONI-La Niña resembles PQDO, but ONI-El Niño shows a different pattern with an opposite sign in the equatorial Pacific. PQDO tends to originate from the subtropical eastern Pacific at year  $-2$ , resembling a Pacific meridional mode-like pattern (Chiang and Vimont 2004). ONI-La Niña bears similarities to PQDO despite the difference in the equatorial eastern Pacific. The similar evolution between PQDO and ONI-La Niña suggests that the low-frequency variability arising from La Niña events may make a critical contribution to the evolution of PQDO.

Between 1878 and 1949, when PQDO was absent, the decadal variability of ONI-El Niño and ONI-La Niña produced similar evolutions (figure S7), suggesting that PQDO would be inactive without La Niña-generated low-frequency variability. We find similar results in the CTRL experiment during the active PQDO epoch (years 1–250) (figure S8).

The simulated evolution of PQDO resembles the observations, suggesting that the model can simulate PQDO.

### 3.2.3. Why the PQDO emerged after 1950 but was absent from 1878 to 1949

We have shown that the La Niña-induced decadal signal makes a significant contribution to PQDO in the ECP. A more profound question remains about what causes La Niña's significant decadal variability, and why is it nonstationary? From 1950 to 2021, the negative phase of PQDO tends to follow the frequent occurrence of multi-year La Niña (figure 1), suggesting that multi-year La Niña events are conducive to reinforcing PQDO.

It is conceivable that the frequent occurrence of multi-year La Niña might be responsible for the emerging PQDO since 1950. The frequency of multi-year La Niña has increased, while the frequency of single-year La Niña events has decreased over the past 144 years. Ten multi-year and five single-year La Niña events occurred between 1950 and 2021. In contrast, there were only three multi-year but 11 single-year events from 1878 to 1949. This change is statistically significant at a 95% confidence level by

**Table 1.** Contingent (two-way) table for testing the statistical significance of the multi-year and single-year La Niña type change around 1950. Two equal-length epochs were compared. The degree of freedom is one, and the chi-square value equals 4.30 ( $p < 0.05$ ).

	Multi-year La Niña type	Single-year La Niña type	Total
1878–1949	3	11	14
1950–2021	10	5	15
Total	13	16	29

the contingency table test (table 1), suggesting that intensification of PQDO since the 1950s is probably due to the change in properties of La Niña.

#### 4. Conclusion and discussion

It has been a great challenge to determine the cause of PQDO in the ECP due to the mixture of heterogeneous internal variability and forced responses in the observations. Our analyses of the 144-year observations and the millennial simulation results from the CESM-LME project shed light on the nonstationary nature and origin of PQDO. Our significant findings are summarized as follows:

- Analysis of the four solar-forcing-only simulation results suggests that 11-year solar irradiance cannot excite PQDO without stratospheric amplification of the solar cycle (figure 2).
- Analysis of the results of both observations and fixed-forcing experiments indicate that PQDO is a nonstationary phenomenon, and internal variability in the coupled climate system could generate PQDO from time to time (figures 3 and 4).
- The internally generated PQDO is primarily shaped by the La Niña-induced decadal variability (figures 3 and 4). The negative phase of PQDO tends to follow the frequent occurrence of multi-year La Niña (figure 1), suggesting that multi-year La Niña events are conducive to generating PQDO.
- Both La Niña and El Niño could induce a significant decadal component. However, La Niña and El Niño possess different SST variability patterns and evolutions (figure 5). The action center forced by La Niña's decadal variability is in the ECP, but the maximum SSTA caused by El Niño's decadal variation is located over the eastern Pacific NINO3.4 region. Therefore, only La Niña's decadal component can reinforce PQDO.
- The intensification of PQDO since 1950s might be primarily due to the increased multi-year La Niña events (table 1). The nonstationarity of PQDO may be rooted in the secular change in the properties of La Niña.

Our findings have ramifications for understanding future changes in PQDO. This work has attributed the emergence of PQDO since the

1950s to the frequent occurrence of multi-year La Niña on a decadal time scale. As shown in figure 3(a), negative PQDO coincides with La Niña events, and the previous consecutive 2-year or 3-year La Niña events correspond to the minima of PQDO. The ongoing (2020–2022) La Niña events (Fang *et al* 2022, Mukhopadhyay *et al* 2022) will probably contribute to a new minimum of PQDO. The observed global warming since the 1950s might have contributed to the increasing trend in multi-year La Niña. However, what makes multi-year La Niña events occur on a decadal time scale remains unknown. These issues deserve further investigation.

Additionally, ENSO and TPDV might be interactive: ENSO could induce low-frequency TPDV, but the ENSO-like TPDV could also impact the Pacific mean-state, changing the relative frequency of the El Niño and La Niña events (Sun and Okumura 2020). There are other unresolved issues. For instance, if PQDO arises from the decadal variation of La Niña, it means an equatorial origin. However, PQDO seems to start from the subtropical northeast Pacific (figure 5(c)). The hypotheses proposed in this work are based on the results from a single-model simulation. More comprehensive multi-model studies are needed to verify the model results.

#### Data availability statement

The HadISST data are available from [www.metoffice.gov.uk/hadobs/hadisst/](http://www.metoffice.gov.uk/hadobs/hadisst/). The ERSST data can be accessed from <https://climatedataguide.ucar.edu/climate-data/sst-data-noaa-extended-reconstruction-ssts-version-5-ersstv5>. The numerical simulation data are obtained from CESM-LME (Otto-Bliesner *et al* 2016) and retrieved from [www.cesm.ucar.edu/projects/community-projects/LME/data-sets.html](http://www.cesm.ucar.edu/projects/community-projects/LME/data-sets.html); the solar forcing used in the CESM-LME is reconstructed by Vieira *et al* (2011) and can be downloaded by the link [www.geosci-model-dev.net/4/33/2011/gmd-4-33-2011-supplement.zip](http://www.geosci-model-dev.net/4/33/2011/gmd-4-33-2011-supplement.zip). Figures were made with NCAR Command Language Version 6.6.2, available at [www.ncl.ucar.edu/Download/](http://www.ncl.ucar.edu/Download/).

All data that support the findings of this study are included within the article (and any supplementary files).

#### Acknowledgments


B W acknowledges support from NSF/Climate Dynamics Award #2025057. This work is jointly supported by the Natural Science Foundation of Xinjiang Uygur Autonomous Region (Grant No. 2022D01C78), the National Natural Science Foundation of China (Grant Nos. 42130604, 41971108, 42075049, 41971021, 42111530182) and the Priority Academic Program Development of Jiangsu Higher Education Institutions (Grant No. 164320H116). This is publication No. 11614 of the School of Ocean

and Earth Science and Technology, publication No. 1589 of the International Pacific Research Center and publication No. 398 of the Earth System Modeling Center.

## Author contributions

C J initialized and wrote the manuscript. B W and J L provided valuable comments and revisions of the manuscript.

## ORCID iD

Chunhan Jin  <https://orcid.org/0000-0002-7048-0906>

## References

- Allan R J 2000 ENSO and climatic variability in the last 150 years *El Niño and the Southern Oscillation: Multiscale Variability, Global and Regional Impacts* ed H F Diaz and V Markgraf (Cambridge: Cambridge University Press) pp 3–55
- Allan R J, Reason C J C, Lindesay J A and Ansell T J 2003 'Protracted' ENSO episodes and their impacts in the Indian Ocean region *Deep Sea Res. Part II* **50** 2331–47
- An S-I and Jin F-F 2004 Nonlinearity and asymmetry of ENSO *J. Clim.* **17** 2399–412
- Anderson B T, Gianotti D J S, Furtado J C and Di Lorenzo E 2016 A decadal precession of atmospheric pressures over the North Pacific *Geophys. Res. Lett.* **43** 3921–7
- Bjerkness J 1969 Atmospheric teleconnections from the equatorial Pacific *Mon. Weather Rev.* **97** 163–72
- Brassington G B 1997 The modal evolution of the Southern Oscillation *J. Clim.* **10** 1021–34
- Bretherton C S, Widmann M, Dymnikov V P, Wallace J M and Bladé I 1999 The effective number of spatial degrees of freedom of a time-varying field *J. Clim.* **12** 1990–2009
- Chiang J C H and Vimont D J 2004 Analogous Pacific and Atlantic meridional modes of tropical atmosphere–ocean variability *J. Clim.* **17** 4143–58
- Drews A, Huo W, Matthes K, Kodera K and Kruschke T 2021 The Sun's role for decadal climate predictability in the North Atlantic *Atmos. Chem. Phys. Discuss.* **2021** 1–17
- Fang X *et al* 2022 Will the historic southeasterly wind over the equatorial Pacific in March 2022 trigger a third-year La Niña event? *Adv. Atmos. Sci.* **40** 6–13
- Huang B, Thorne P W, Banzon V F, Boyer T, Chepurin G, Lawrimore J H, Menne M J, Smith T M, Vose R S and Zhang H-M 2017 Extended reconstructed sea surface temperature, version 5 (ERSSTv5): upgrades, validations, and intercomparisons *J. Clim.* **30** 8179–205
- Huo W, Xiao Z, Wang X and Zhao L 2021 Lagged responses of the tropical Pacific to the 11-yr solar cycle forcing and possible mechanisms *J. Meteorol. Res.* **35** 444–59
- Jin C, Wang B and Liu J 2021 Emerging Pacific quasi-decadal oscillation over the past 70 years *Geophys. Res. Lett.* **48** e2020GL090851
- Kim G-I and Kug J-S 2020 Tropical Pacific decadal variability induced by nonlinear rectification of El Niño–Southern Oscillation *J. Clim.* **33** 7289–302
- Li G, Xie S-P, Du Y and Luo Y 2016 Effects of excessive equatorial cold tongue bias on the projections of tropical Pacific climate change. Part I: the warming pattern in CMIP5 multi-model ensemble *Clim. Dyn.* **47** 3817–31
- Lyu K, Zhang X, Church J A, Hu J and Yu J-Y 2017 Distinguishing the quasi-decadal and multidecadal sea level and climate variations in the Pacific: implications for the ENSO-like low-frequency variability *J. Clim.* **30** 5097–117
- Mantua N J, Hare S R, Zhang Y, Wallace J M and Francis R C 1997 A Pacific interdecadal climate oscillation with impacts on salmon production *Bull. Am. Meteorol. Soc.* **78** 1069–80
- Meehl G A and Arblaster J M 2009 A lagged warm event-like response to peaks in solar forcing in the Pacific region *J. Clim.* **22** 3647–60
- Meehl G A, Arblaster J M, Matthes K, Sassi F and van Loon H 2009 Amplifying the Pacific climate system response to a small 11-year solar cycle forcing *Science* **325** 1114–8
- Misios S, Gray L J, Knudsen M F, Karoff C, Schmidt H and Haigh J D 2019 Slowdown of the Walker circulation at solar cycle maximum *Proc. Natl Acad. Sci.* **116** 201815060
- Misios S and Schmidt H 2012 Mechanisms involved in the amplification of the 11-yr solar cycle signal in the tropical Pacific Ocean *J. Clim.* **25** 5102–18
- Monahan A H and Dai A 2004 The spatial and temporal structure of ENSO nonlinearity *J. Clim.* **17** 3026–36
- Mukhopadhyay S, Gnanaseelan C, Chowdary J S, Parekh A and Mohapatra S 2022 Prolonged La Niña events and the associated heat distribution in the tropical Indian Ocean *Clim. Dyn.* **58** 2351–69
- Okumura Y M and Deser C 2010 Asymmetry in the duration of El Niño and La Niña *J. Clim.* **23** 5826–43
- Otto-Bliesner B L, Brady E C, Fasullo J, Jahn A, Landrum L, Stevenson S, Rosenbloom N, Mai A and Strand G 2016 Climate variability and change since 850 CE: an ensemble approach with the community earth system model *Bull. Am. Meteorol. Soc.* **97** 735–54
- Power S *et al* 2021 Decadal climate variability in the tropical Pacific: characteristics, causes, predictability, and prospects *Science* **374** eaay9165
- Power S, Casey T, Folland C, Colman A and Mehta V 1999 Inter-decadal modulation of the impact of ENSO on Australia *Clim. Dyn.* **15** 319–24
- Rasmusson E M and Carpenter T H 1982 Variations in tropical sea surface temperature and surface wind fields associated with the Southern Oscillation/El Niño *Mon. Weather Rev.* **110** 354–84
- Rayner N A *et al* 2003 Global analyses of sea surface temperature, sea ice, and night marine air temperature since the late nineteenth century *J. Geophys. Res.* **108** 4407
- Roy I and Haigh J D 2010 Solar cycle signals in sea level pressure and sea surface temperature *Atmos. Chem. Phys.* **10** 3147–53
- Sun T and Okumura Y M 2020 Impact of ENSO-like tropical Pacific decadal variability on the relative frequency of El Niño and La Niña Events *Geophys. Res. Lett.* **47** e2019GL085832
- Tourre Y M, Rajagopalan B, Kushnir Y, Barlow M and White W B 2001 Patterns of coherent decadal and interdecadal climate signals in the Pacific basin during the 20th century *Geophys. Res. Lett.* **28** 2069–72
- Tung K-K and Zhou J 2010 The Pacific's response to surface heating in 130 yr of SST: La Niña-like or El Niño-like? *J. Atmos. Sci.* **67** 2649–57
- Van Loon H, Meehl G A and Shea D J 2007 Coupled air–sea response to solar forcing in the Pacific region during northern winter *J. Geophys. Res.* **112** D2108
- Vieira L E A, Solanki S K, Krivova N A and Usoskin I 2011 Evolution of the solar irradiance during the Holocene *Astron. Astrophys.* **531** A6
- Vimont D J 2005 The contribution of the interannual ENSO cycle to the spatial pattern of decadal ENSO-like variability *J. Clim.* **18** 2080–92
- Wang B, Luo X, Yang Y-M, Sun W, Cane M A, Cai W, Yeh S-W and Liu J 2019 Historical change of El Niño properties sheds light on future changes of extreme El Niño *Proc. Natl Acad. Sci.* **116** 22512–7
- Wang S, Hakala K, Gillies R R and Capehart W J 2014 The Pacific quasi-decadal oscillation (QDO): an important precursor toward anticipating major flood events in the Missouri River Basin? *Geophys. Res. Lett.* **41** 991–7
- White W B, Cayan D R and Lean J 1998 Global upper ocean heat storage response to radiative forcing from changing solar

- irradiance and increasing greenhouse gas/aerosol concentrations *J. Geophys. Res.* **103** 21355–66
- White W B and Liu Z 2008a Non-linear alignment of El Nino to the 11-yr solar cycle *Geophys. Res. Lett.* **35** L19607
- White W B and Liu Z 2008b Resonant excitation of the quasi-decadal oscillation by the 11-year signal in the Sun's irradiance *J. Geophys. Res.* **113** C01002
- White W B, Tourre Y M, Barlow M and Dettinger M 2003 A delayed action oscillator shared by biennial, interannual, and decadal signals in the Pacific Basin *J. Geophys. Res.* **108** 3070
- Wittenberg A T 2009 Are historical records sufficient to constrain ENSO simulations? *Geophys. Res. Lett.* **36** L12702
- Ying J, Huang P, Lian T and Tan H 2019 Understanding the effect of an excessive cold tongue bias on projecting the tropical Pacific SST warming pattern in CMIP5 models *Clim. Dyn.* **52** 1805–18
- Yue S, Wang B, Yang K, Xie Z, Lu H and He J 2020 Mechanisms of the decadal variability of monsoon rainfall in the southern Tibetan Plateau *Environ. Res. Lett.* **16** 014011
- Zhao Y and Di Lorenzo E 2020 The impacts of extra-tropical ENSO precursors on tropical Pacific decadal-scale variability *Sci. Rep.* **10** 3031